Evaluation of the Hurricane Research Division Doppler Radar Analysis Software Using Synthetic Data

SYLVIE LORSOLO

Cooperative Institute of Marine and Atmospheric Studies, Rosenstiel School of Marine and Atmospheric Science, University of Miami, and Hurricane Research Division, NOAA/AOML, Miami, Florida

JOHN GAMACHE

Hurricane Research Division, NOAA/AOML, Miami, Florida

ALTUG AKSOY

Cooperative Institute of Marine and Atmospheric Studies, Rosenstiel School of Marine and Atmospheric Science, University of Miami, and Hurricane Research Division, NOAA/AOML, Miami, Florida

(Manuscript received 14 August 2012, in final form 21 November 2012)

ABSTRACT

The Hurricane Research Division Doppler radar analysis software provides three-dimensional analyses of the three wind components in tropical cyclones. Although this software has been used for over a decade, there has never been a complete and in-depth evaluation of the resulting analyses. The goal here is to provide an evaluation that will permit the best use of the analyses, but also to improve the software. To evaluate the software, analyses are produced from simulated radar data acquired from an output of a Hurricane Weather Research and Forecasting (HWRF) model nature run and are compared against the model ''truth'' wind fields. Comparisons of the three components of the wind show that the software provides analyses of good quality. The tangential wind is best retrieved, exhibiting an overall small mean error of 0.5 m s^{-1} at most levels and a root-mean-square error less than 2 m s^{-1}. The retrieval of the radial wind is also quite accurate, exhibiting comparable errors, although the accuracy of the tangential wind is generally better. Some degradation of the retrieval quality is observed at higher altitude, mainly due to sparser distribution of data in the model. The vertical component of the wind appears to be the most challenging to retrieve, but the software still provides acceptable results. The tropical cyclone mean azimuthal structure and wavenumber structure are found to be very well captured. Sources of errors inherent to airborne Doppler measurements and the effects of some of the simplifications used in the simulation methodology are also discussed.

1. Introduction

The concept of using airborne Doppler radars to obtain observations of the three-dimensional wind field was first described over 40 years ago (Lhermitte 1971) and first tested 12 years later (Jorgensen et al. 1983). Since then, the concept has evolved into a working technology and has been widely employed in scientific projects such as the Verification of the Origins of Rotation in Tornadoes Experiment (VORTEX; Wakimoto et al. 1996) and the Intensity Forecasting Experiment (IFEX; Rogers et al. 2006) to investigate various atmospheric phenomena.

The Hurricane Research Division (HRD) of the National Oceanic and Atmospheric Administration (NOAA) has been collecting such data in tropical cyclones (TCs) for three decades using the tail Doppler radars installed on the WD-P3 (P3) aircraft (e.g., Jorgensen et al. 1983; Marks 2003). During this period, various methods of analysis have been used in an effort to retrieve the three-dimensional wind field as accurately as possible. At first, the single scanning direction of the tail radar required a flight track during which the aircraft followed two orthogonal paths (Jorgensen et al. 1983) to allow what is called a pseudo-dual-Doppler

Corresponding author address: Sylvie Lorsolo, Hurricane Research Division, NOAA/AOML, 4301 Rickenbacker Cswy., Miami, FL 33149-1097.
E-mail: sylvie.lorsolo@noaa.gov

DOI: 10.1175/JTECH-D-12-00161.1

© 2013 American Meteorological Society

Unauthenticated | Downloaded 04/25/25 07:24 PM UTC

analysis. Indeed, with such a flight track, the storm can be sampled from different viewing angles. This then allows retrieval of the three-dimensional wind using the dual-Doppler retrieval technique. The method required a long time between the acquisition of two intersecting Doppler radial rays and thus impeded good temporal resolution for the resulting three-dimensional wind retrieval. Comparison with ground-based radar showed promising results, although the coarser temporal and spatial resolution of the ground radar could not allow for optimal comparison in localized regions of the sampled storm. Jorgensen et al. (1983) assessed other sources of errors of the wind retrieval, including the use of horizontal convergence to derive the vertical component of the wind, which was found to potentially lead to large errors. Aircraft position and attitude and radar sidelobe effects were other sources of error.

The new method was nevertheless successfully implemented and allowed, for the first time, for a detailed mapping of the horizontal wind of Hurricane Debbie (1982) (Marks and Houze 1984). A few years later, an analysis of the three-dimensional wind of Hurricane Alicia (1983) (Marks and Houze 1987) was performed, starting a new era of research on hurricane kinematic structure (Marks 2003). Over the years, the use of the tail Doppler radar was improved. To alleviate the resolution issue, a second radar was installed on the other NOAA P3 and both radars were flown together (Dodge et al. 1999; Reasor et al. 2000; Gamache et al. 1995). The fore/aft scanning technique (FAST) was also implemented (Jorgensen and DuGranrut 1991) for the first time. Both upgrades allowed for improved retrieval of the three-dimensional wind field (Jorgensen et al. 1996; Gamache et al. 1995), and it was determined that FAST was the most effective method to retrieve an accurate kinematic representation of a TC inner core (~200 km from the TC center), as it only required the use of one aircraft.

Along with the acquisition techniques, much effort was also made to improve and optimize the wind retrieval algorithms. Because the airborne radars are installed on moving platforms, retrieval of the wind components is more complex than for ground-based radars. Lee et al. (2003) provides a detailed description of the background of the wind retrieval using airborne radar data. Variational techniques (Ray et al. 1980; Bousquet and Chong 1998; Gao et al. 1999) are commonly used in three-dimensional wind retrievals (Gamache 1997; Reasor et al. 2000; Gao et al. 1999) and have been proven successful (Gamache 1997; Reasor et al. 2000, 2009).

Radar analysis procedures require the data to be first edited to remove bad measurements inherent to Doppler radar technology (ground clutter, sidelobes, etc.). Automatic quality control has thus become necessary to improve radar processing efficiency and accessibility. For this purpose, HRD developed an automatic analysis software, which contains three main steps:

- Automatic quality control: Dealiasing, erroneous data removal and navigation correction (Testud et al. 1995);
- Interpolation to a Cartesian grid centered on the center of circulation, as described in Reasor et al. (2009);
- Synthesis: The actual three-dimensional wind retrieval procedure using a variational method (Gamache 1997; Gao et al. 1999).

The automatic software has provided high-quality, three-dimensional analyses that have allowed for detailed documentation of the hurricane kinematic structure (Reasor et al. 2000, 2009; Rogers et al. 2012; Lorsolo et al. 2010). Reasor et al. (2000, 2009) conducted thorough studies to better understand the impact of shear on inner-core structure using the three-dimensional analyses. However, both studies only used the last two steps of the software, as manual editing was performed in these cases. Rogers et al. (2012) provided a detailed composite analysis of the hurricane inner core using analyses produced from the full automatic software. Lorsolo et al. (2010) were able to estimate the turbulent kinetic energy of hurricanes using a variant of the software.

Meanwhile, one of the main efforts in hurricane research has recently focused on a better evaluation of new high-resolution mesoscale models increasingly used in operations, such as the Hurricane Weather Research and Forecasting (HWRF) numerical model (X. Zhang et al. 2011; Gopalakrishnan et al. 2011). One efficient tool for such a task is the set of Doppler radar analyses produced using analysis software such as HRD's. These analyses can be useful to diagnose model performance as well as evaluate parameterization packages, especially for the hurricane's inner core. Stern and Nolan (2009) made use of Doppler analyses from the P3 tail Doppler radar to evaluate numerical model data.

To enable a wide use of the retrieved winds, the retrieval needs to be accurate, and thus carefully assessed. Over the years, various studies have evaluated the quality of the retrieved winds using independent sources, such as ground-based radar data (Hildebrand and Mueller 1985; Ray and Jorgensen 1988; Ray and Stephenson 1990) or in situ measurements such as flight-level data (Reasor et al. 2009; Lorsolo et al. 2010; Marks et al. 1992). It was generally found that the retrieved data were of good quality. However, to obtain an accurate estimation of errors in the retrieval and to allow for a wider use of the analyses, a more detailed evaluation is needed. Unfortunately, comparison using ground-based radar data can be challenging because of different resolution and sensitivity of the radars. Other

Unauthenticated | Downloaded 04/25/25 07:24 PM UTC

types of aircraft data (flight-level data, dropwindsonde, etc.) are point measurements, while radar data are beam-volume samples, making any comparison problematic. The use of synthetic data, where the ''truth'' is known, allows for a more comprehensive assessment of the quality of the three-dimensional wind retrieval. This evaluation technique was first performed by Gamache (1997), where a three-dimensional analytic field was generated. The analytic signal was defined based on the fact that any signal is composed of the sum of sine and cosine functions with specific wavelengths in the azimuthal direction. The horizontal wavelength of the analytic field was set at two values, 10 and 25 km, whereas the vertical wavelength was set at 15 km. It was found that the interpolation scheme caused most of the resulting errors in the both the 10- and 25-km wavelength cases. It was also revealed that the analysis had less, but still acceptable, accuracy when radial rays greater than 45° from the horizontal were included in the retrieval. Although the study provided an accurate assessment of the analysis software, it did not provide a complete assessment of the errors related to the nature of the data sampled. Indeed, the simulated field did not have as high spatial gradients as in real wind fields; it did not have noise and multiple scales of motion similar to that of real radar data; and radial measurements were assumed to exist everywhere in the field, thus assuming that there were no missing data in the simulated observations.

The goal of this study is to extend the results of Gamache (1997) to assess and improve the retrieval method in a framework where issues inherent to real wind fields are taken into account. In this study, synthetic observations are generated from an observing system simulation experiment (OSSE) (Aksoy et al. 2012, hereafter A12), by simulating a realistic track and scanning strategy from a NOAA P3 tail Doppler radar through a TC. A wind field with various scales of motion (e.g., a wind field composed of multiple azimuthal wavenumbers relative to the storm center) and missing data are thus part of the simulated Doppler radial measurements, making the data quite realistic. The wind field is then retrieved using the automatic analysis software and a comparison of the resulting analysis field with the truth field (i.e., the HWRF model field) is performed. Although the experiment is meant to duplicate as much as possible what happens during the real data collection, navigation errors, sidelobes, ground clutter, and beamfilling are not simulated and thus the automatic quality control step is bypassed.

This paper is organized as follows: Section 2 provides a description of the simulated data collection, and overviews of the software analysis and model from which the data are generated. In section 3 a complete evaluation of the retrieved winds is performed, and section 4 discusses error sources and the impact of simplifications in the methodology. Finally, section 5 provides a summary and conclusions.

2. Experiment

Only Doppler radial velocities are simulated in this study and are obtained from wind velocities rather than precipitation velocities. Indeed, the model used to obtain the simulated data does not contain reflectivity as a variable and HRD has not yet developed a forward operator to retrieve reflectivity. Consequently, fall velocities, usually weighted by reflectivity, are not simulated. The Doppler radial rays are generated from a simulated flight track across a model field from a nature run simulation of Hurricane Paloma (2008) that has realistic TC characteristics (A12). The horizontal resolution of the model domain from which Doppler radial measurements are simulated is 1.5 km. For a complete description of the model and the model run refer to Gopalakrishnan et al. (2011) and A12, respectively. The simulated track is designed to have characteristics similar to that of the P3 in real time. The aircraft is set to fly an hour as in a real TC penetration, at an altitude of 3 km with a ground speed of 115 m s^{-1}, flying due east across the field. The simulated radar performs the same FAST scanning with similar antenna rotation (10 rpm). Once the position of the radial bins is determined, the Doppler radial values are computed using the model wind field. First, the model wind components are interpolated to the radial bin positions, and then the Doppler radial velocities are computed as projections of the model wind vectors onto the simulated radial rays. The resulting Doppler radial line-of-sight velocities (LOSVs) are set to have the same gate-to-gate resolution as the actual radar. A complete description of the generation of the simulated radial LOSV is provided in A12. Attitude angles (drift, pitch, and roll) are kept at a value of zero for simplicity.

A threshold on cloud water content (7.5×10^{-5} g kg^{-1}) is applied to simulate areas where a lack of reflectors would result in missing data in reality. The simulated flight track and horizontal and vertical distribution of data are shown in A12 (their Fig. 8). The data used in the present study are taken from the first (east–west) leg, at the center time of the assimilation period.

Once the Doppler radial LOSVs are simulated, they are then used in the HRD analysis software to produce the three-dimensional wind analysis. The processing that produces the resulting wind analysis is slightly different from the one used in real time. The simulated data are initially spatially referenced in an Earth-relative framework, and thus conversion to aircraft-relative framework

Unauthenticated | Downloaded 04/25/25 07:24 PM UTC

(Lee et al. 1994) is first performed. Because none of the data collection issues inherent to Doppler radar data is simulated (ground clutter, second-trip echo, etc.), no data quality control is performed (Reasor et al. 2009). The retrieval procedure involves interpolation of the data and synthesis of the wind field. To run the interpolation scheme, a few parameters need to be fixed, such as the center time of the analysis, horizontal and vertical information for the *e*-folding distance for the Gaussian interpolation (2 and 0.5 km, respectively), and the maximum distance from a grid point for an observation to be included in the interpolation (4 and 1 km, respectively).

Once the interpolation is completed, the wind synthesis can be performed. Parameters such as height and size of the melting layer, convergence parameters of the variational method, and the continuity constraint are provided. For this experiment, no background (first guess) field was used. Because a single time step of the model output was used during the simulation, there was no change in the storm structure between the start and the end of the simulated flight, thus no advection component was added during the interpolation process. Moreover, since the simulated data are obtained from the components of the full wind, it is not necessary to remove the fall speed. The same smoothing procedure (Gao et al. 1999) as in real time is used here. A least squares fit is applied, where the cost function includes 1) the deviation from the fourth-order difference representation of mass continuity (high weight), 2) the difference between the observed Doppler radial velocity and the projection of the wind on the Doppler radial pointing direction (moderate weight), 3) the fourth-order second derivative of the wind components (low weight), and 4) the difference between the vertical wind speed (hereafter vertical wind) at the vertical boundaries and zero (moderate weight).

The resulting three-dimensional wind field is situated on a Cartesian grid with a uniform horizontal and vertical resolution of 2 and 0.5 km, respectively, and is centered on the storm center. Thirty-six vertical levels are represented starting at 500 m above mean sea level (MSL). To obtain a one-to-one comparison of the three wind components of the resulting wind analysis with the model (hereafter truth) data, the truth data are interpolated to a Cartesian grid with the same resolution as the analysis data.

3. Evaluation

a. Wind components evaluation

1) TANGENTIAL WIND COMPONENT

A one-to-one comparison is performed to evaluate the quality of the retrieved winds in the analysis compared to the truth. Figure 1 shows the tangential wind component of the horizontal wind for both the truth (left column) and the analysis (right column) at 1, 4, and 8 km MSL. The truth fields are presented using the cloud water content (CWC) threshold used to simulate the radar data so that one can have an idea of what the actual sampled field looks like. However, statistics for the truth data are computed using the entire wind field, since the purpose of this study is to compare the analysis with the actual truth field. The comparison shows an overall good agreement between the fields. The maxima are correctly retrieved spatially and even some small-scale features, such as the one at 1 km MSL east of the center, are well captured in the analysis. In general, the retrieved field is somewhat smoother than the true field, due to the smoothing involved in the processing. The interpolation algorithm allows partial retrieval of the wind field at grid points with missing data. The strongest agreement is found at lower levels, where there are fewer missing data. This suggests that the retrieval accuracy is impacted negatively by the amount of the missing data. The largest errors are in the eye, where there are not enough reflectors to allow for an adequate sampling. Edges of areas of missing data also tend to display larger errors, since the solution is less accurate at the boundaries.

The frequency distribution of errors (Fig. 2, left column) exhibits a well-defined bell shape with a slight negative bias at 1 km MSL, a slight positive bias at 4 km MSL and a larger one at 8 km MSL. Although small in magnitude, the biases are statistically significant at the 95% confidence interval, using the bootstrap method and could be due to the methodology used while integrating the continuity equation (see section 4 for a more detailed explanation).

Figure 3a presents the variation of the mean error of tangential wind with height up to 13 km MSL (above 13 km, the data coverage was too limited to provide a reliable retrieval). There is a negative bias below 3 km MSL and a positive bias above 3 km MSL, indicating an underestimation of the tangential wind below 3 km MSL and overestimation above. In general, the mean error remains rather small (<0.5 m s^{-1}) at most levels. Figure 3b presents the root-mean-square error (RMSE). The most accurate retrieval is obtained at the lowest levels. The RMSE increases steadily with height, yet remains small (<2 m s^{-1}). Overall, the retrieval of the tangential wind component is quite accurate.

2) RADIAL WIND COMPONENT

Evaluation of the radial wind component is presented. Figure 4 is similar to Fig. 1 but for the radial wind. Similar to the tangential wind field, the analysis field is

Unauthenticated | Downloaded 04/25/25 07:24 PM UTC

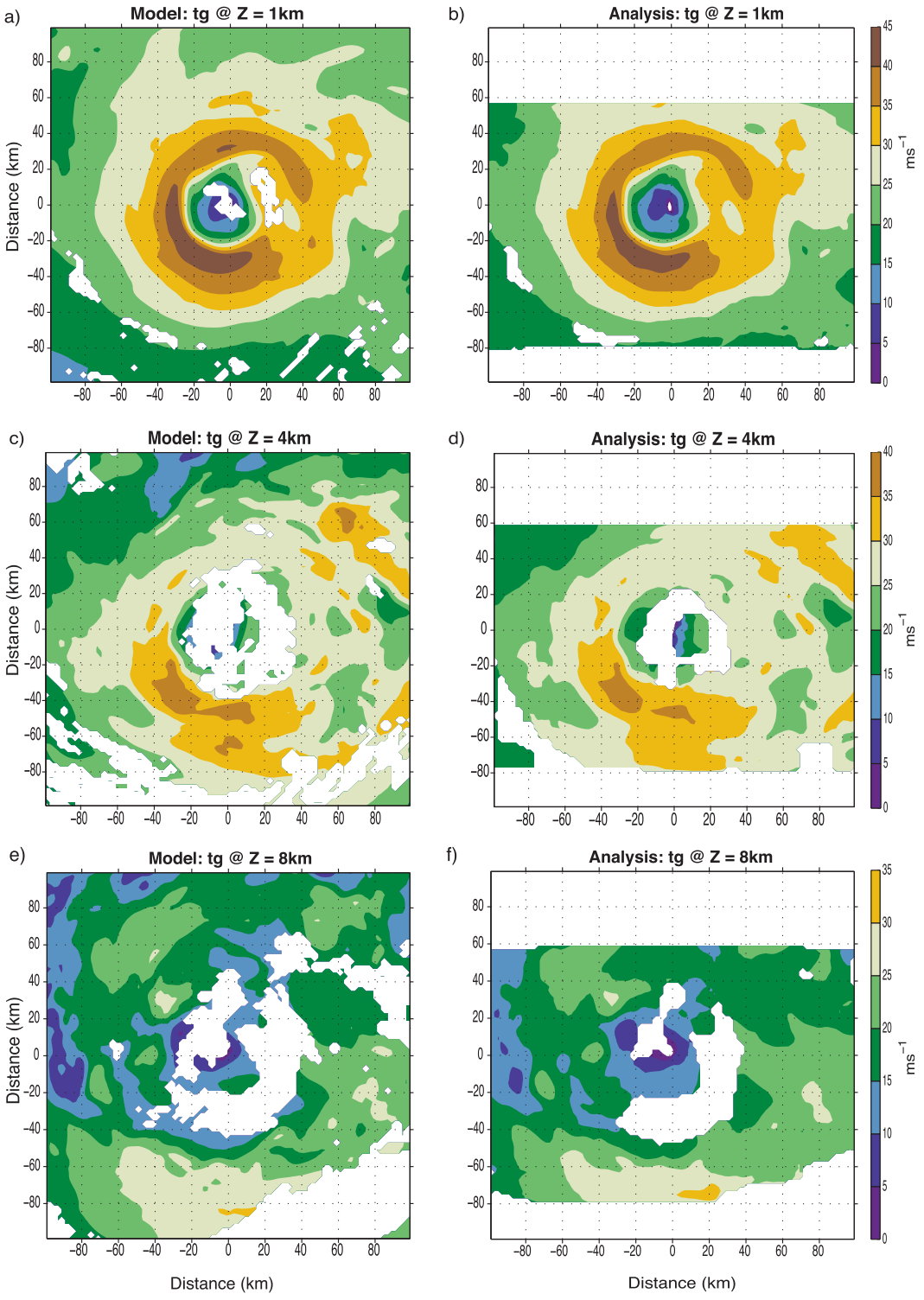

FIG. 1. Horizontal cross sections of the tangential wind component from the (left) truth and (right) Doppler radar analysis at (top) 1, (middle) 4, and (bottom) 8 km MSL.

Unauthenticated | Downloaded 04/25/25 07:24 PM UTC

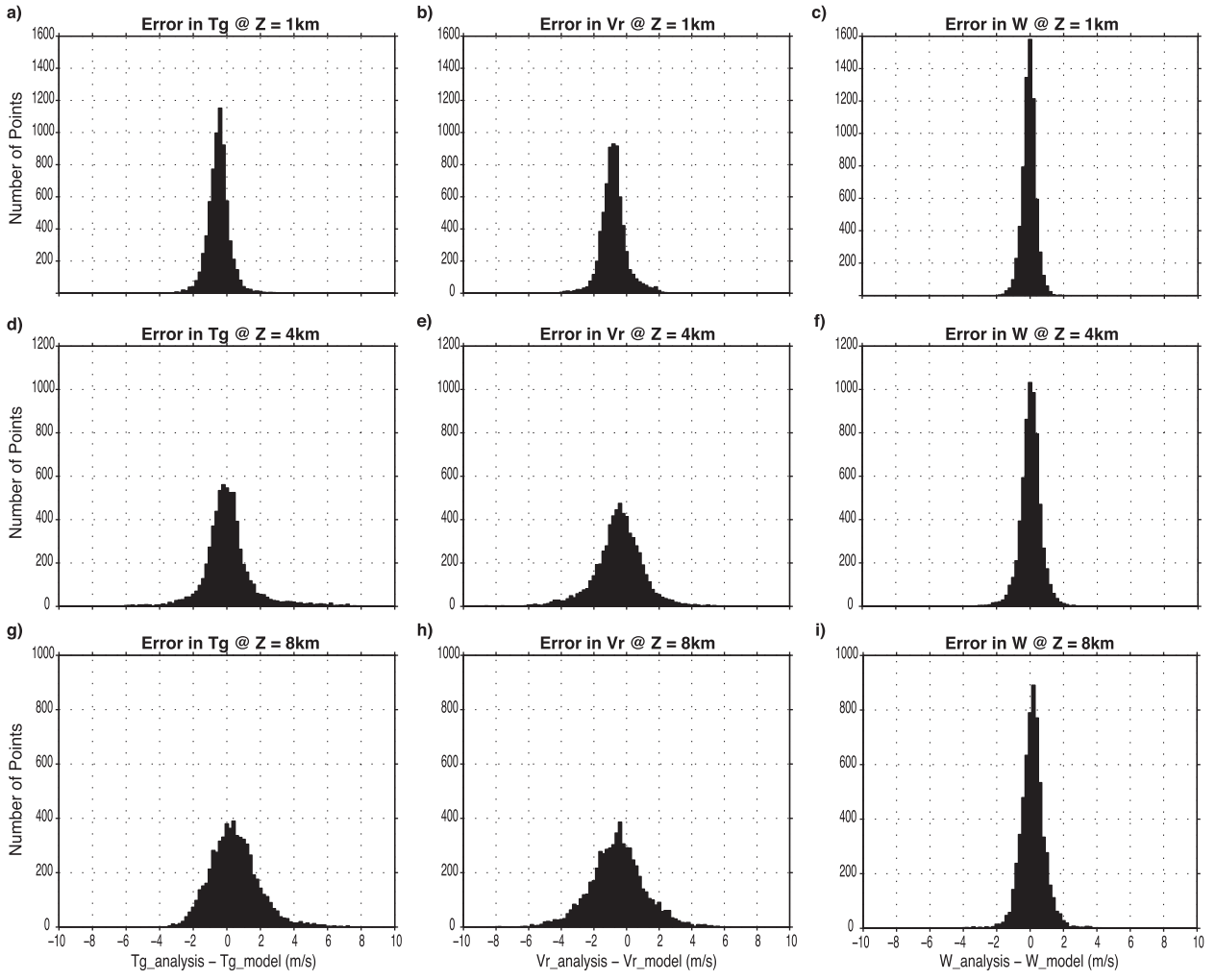

FIG. 2. Distribution of error in the (left) tangential, (middle) radial, and (right) vertical wind component retrieval at (top) 1, (middle) 4, and (bottom) 8 km MSL.

smoother, exhibiting fewer small-scale details of the original radial wind field. However, there is a good general agreement between the truth and the analysis. Here, the upward loss of accuracy is more subtle but is also present. It is evident that, just as with the tangential wind, there is an underestimation of the radial wind, except for the area near the center. The error distribution (Fig. 2, middle column) at all levels exhibits a bell shape, getting wider with height, confirming the increase of the error with height. In the case of the radial wind, there is a negative bias at all levels, which means that the analysis underestimates the outflow circulation (positive radial wind) and/or overestimates the inflow circulation (negative radial wind). Note that the bias is smallest at the lowest levels, where the inflow is the strongest, and thus should not affect the interpretation of the low-level processes. This bias is also shown in Fig. 3a, which documents the evolution of the mean error with height, confirming a general negative bias of around 0.5 m s^{-1}. The RMSE of the radial wind (Fig. 3b) is generally greater than that of the tangential wind, suggesting that the retrieval is slightly less accurate for the radial wind. The negative bias and generally larger RMSEs could be due to the radial trajectory of the plane. Indeed, the tangential wind is measured more directly than the radial wind by the Doppler radar due to the radial trajectory of the plane when sampling the storm (Gamache et al. 1995). However, the RMSE of the radial wind data is still generally small, which implies a rather accurate retrieval.

3) VERTICAL WIND COMPONENT

Figure 5 presents the comparison between the truth and the analysis for the vertical component of the wind as in Figs. 1 and 4. Unlike before, the strongest agreement is not found at the lowest level, which is due to the weaker weight imposed at the lower boundary of the

Unauthenticated | Downloaded 04/25/25 07:24 PM UTC

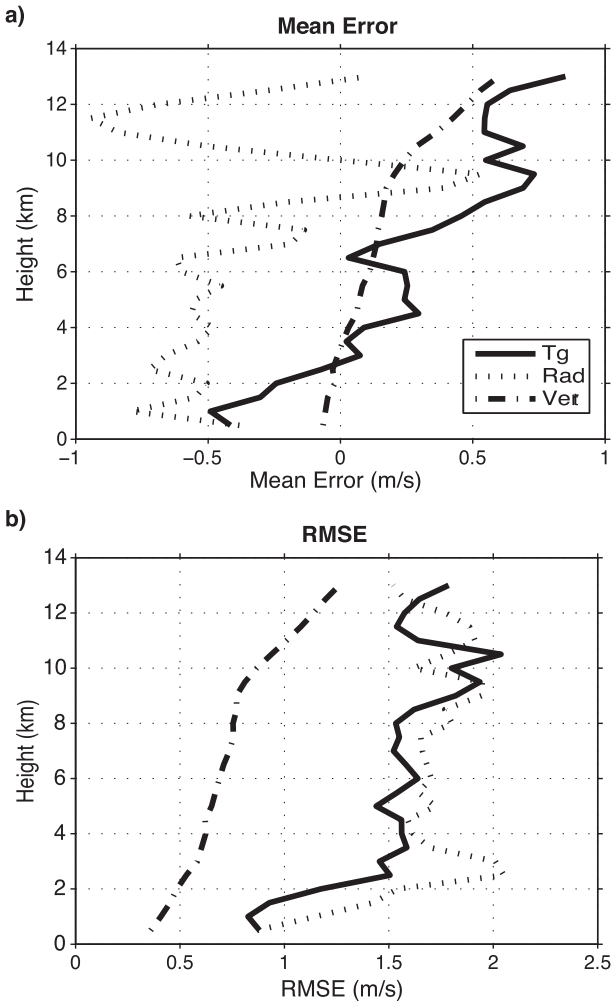

FIG. 3. Evolution with height of the (a) mean error and (b) RMSE of the retrieval for the tangential wind (solid), the radial wind (dotted), and the vertical wind (dash–dotted).

domain. At 1 km MSL, the analysis presents some similarities to the truth but appears noisier. The updraft near the eyewall appears weaker in the analysis, while the downdraft appears stronger. The analysis exhibits small errors compared to those seen for the horizontal components of the winds, which is due to the smaller magnitude of gradients in the vertical wind field. At 4-km height, the truth and analysis data are much more consistent, although the smoothing in the analysis appears to make the small-scale features broader. The main updrafts appear weaker and the downdrafts stronger also at this height. This discrepancy is likely due to the inherent characteristics of the vertical wind retrieval. Indeed, although the solution is fully three dimensional through most of the domain, the vertical component of the wind is most highly dependent upon the integration of divergence over a small domain (Marks et al. 1992). Thus, evaluating the vertical motion through gridpoint-by-gridpoint comparison could be a bit of an unfair comparison.

A spurious feature in the analysis, at the lowest level (identified by the box in Fig. 5b), appears to extend upward, getting stronger while doing so. The feature does not seem to be present in the truth field; however, evaluation of a more detailed representation of the truth field (not shown here) exhibits a feature similar with a much weaker amplitude but only at 4 km MSL. Missing upper-level data and a strong gradient in radial wind may combine with the continuity equation integration to produce these erroneous vertical wind values.

As for the horizontal components of the wind, the error distribution of the vertical component of the wind (Fig. 2, right column) at 1 km MSL is narrower than at higher levels. The error distribution is a little skewed toward the negative, confirming that updrafts (downdrafts) are mostly weaker (stronger) in the analysis. The skewness shifts slightly to the positive with height, and the distribution becomes wider when data become sparser, as seen for tangential and radial wind components. Figure 3a presents the variation of the vertical wind mean error with height. There is a negative bias in the vertical wind below 3 km MSL (altitude of the radar) and a positive bias above where large areas of positive vertical motion are seen (not shown here). The error in vertical wind becomes significantly larger above 8 km MSL. Unlike the radial and tangential components, the RMSE (Fig. 3b) follows a steep increase with height, with values smaller than those computed for the other components.

Because it is evident that the retrieval of the vertical component of the wind is less accurate than that of the horizontal wind, the RMSE is normalized to allow for a more comprehensive comparison between variables. Here, the normalized RMSE (NRMSE) is defined as

$$\mathrm{NRMSE}(z) = \frac{\mathrm{RMSE}(z)}{\mathrm{Max}_{\mathrm{model}}(z) - \mathrm{Min}_{\mathrm{model}}(z)},$$

where $\mathrm{Max}_{\mathrm{model}}(z)$ and $\mathrm{Min}_{\mathrm{model}}(z)$ are the maximum and the minimum values of the considered variable at each height z, respectively. Essentially, the RMSE is normalized by the magnitude of the range of the truth data for a given level. The normalized RMSE is a nondimensional variable. Figure 6 presents the variation of the normalized RMSE with increasing height for tangential (solid), radial (dotted), and vertical (dashed) wind components. The NRMSE for both the tangential and radial wind components follows a similar pattern to that of RMSE. Meanwhile, NRMSE for the vertical

Unauthenticated | Downloaded 04/25/25 07:24 PM UTC

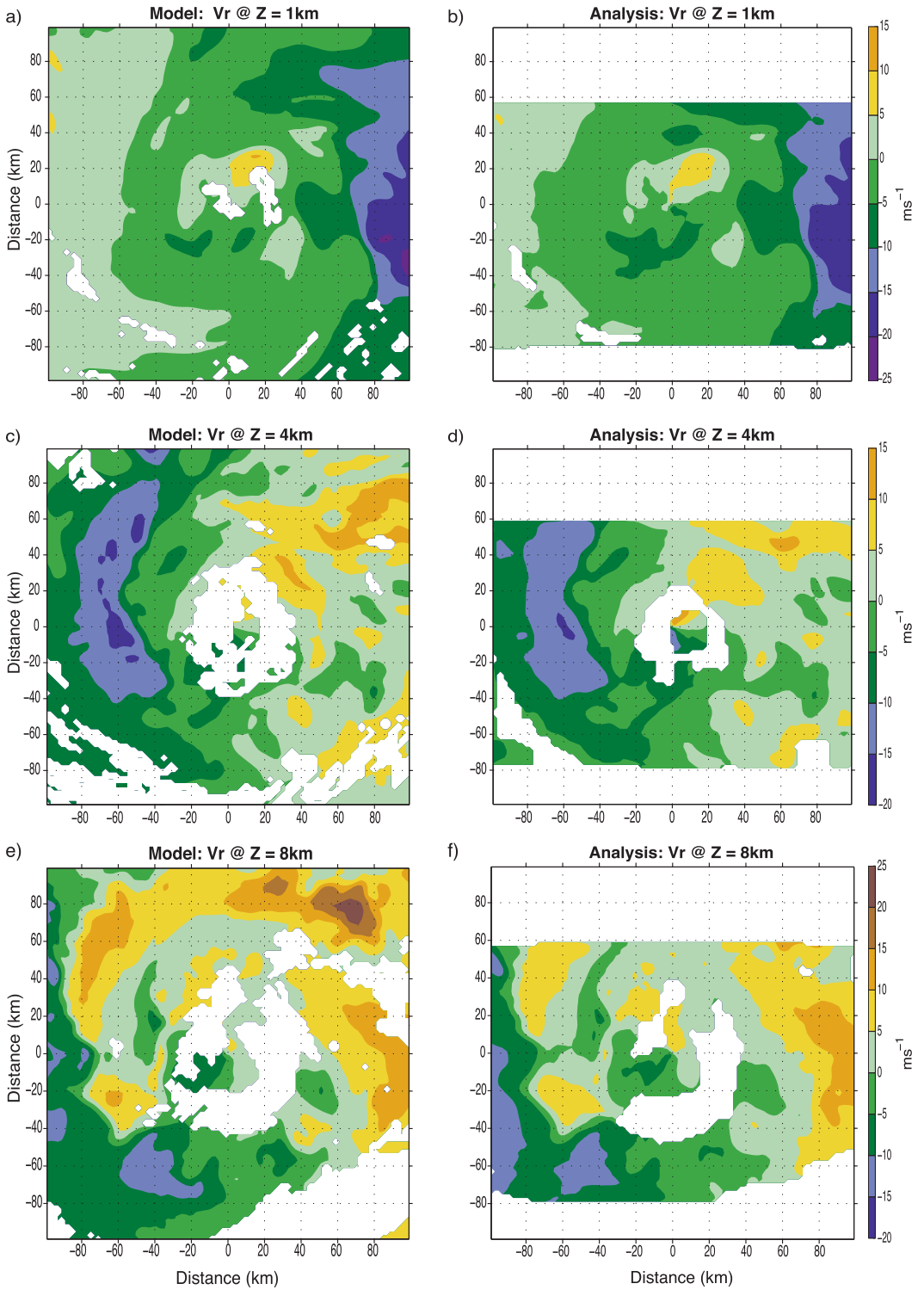

FIG. 4. As in Fig. 1, but for the radial wind component.

wind behaves significantly different from RMSE. Indeed, unlike RMSE, NRMSE first decreases with height, which is consistent with the better retrieval at midlevels as documented in Fig. 3. The normalized RMSEs then remain nearly constant except between 7 and 9 km MSL, where the truth range values suddenly decease (not shown). Overall, as expected, the normalized RMSE of the vertical wind component is larger

Unauthenticated | Downloaded 04/25/25 07:24 PM UTC

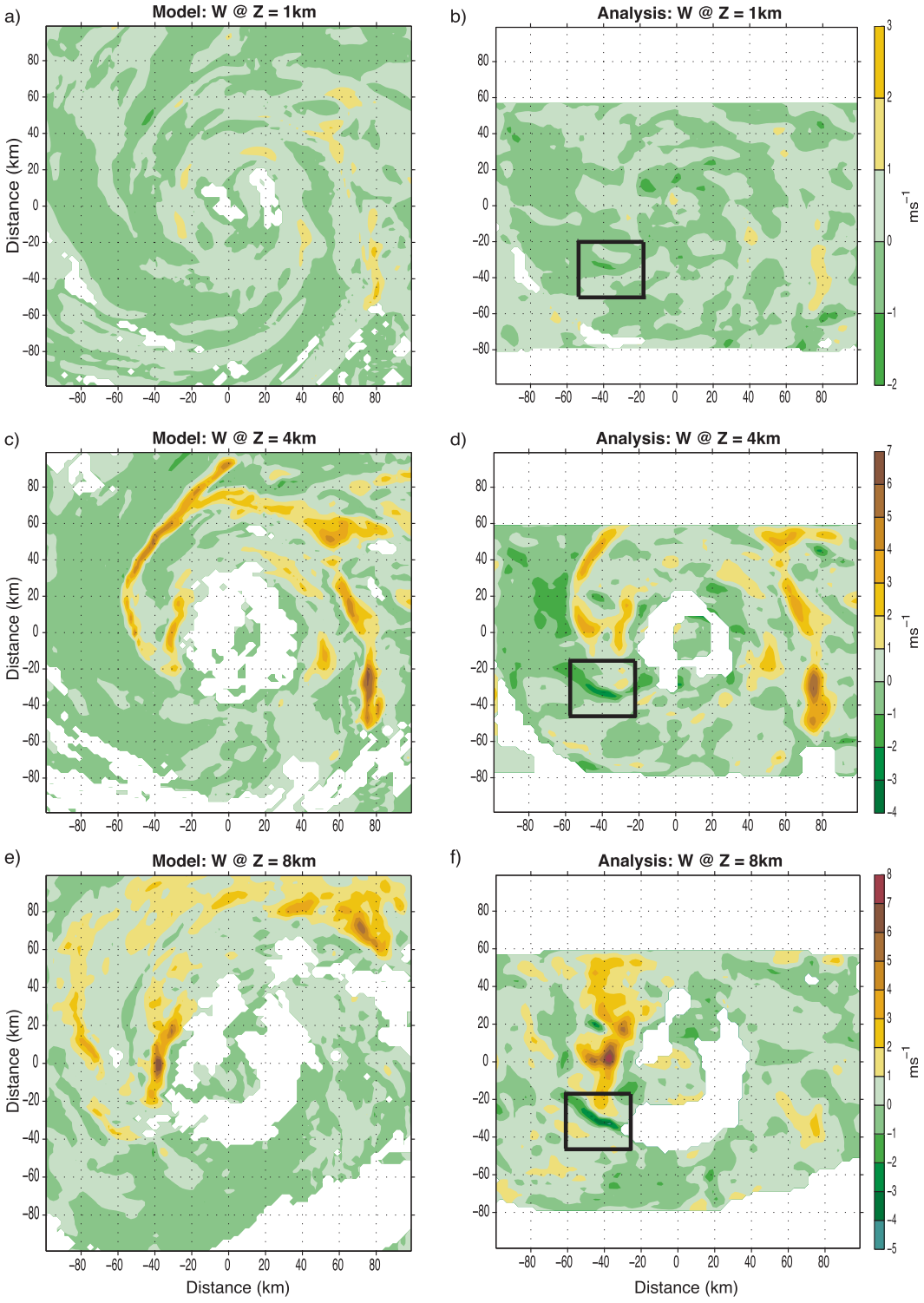

FIG. 5. As in Fig. 1, but for the vertical wind component. Black box identifies a spurious feature existing in the vertical wind field.

Unauthenticated | Downloaded 04/25/25 07:24 PM UTC

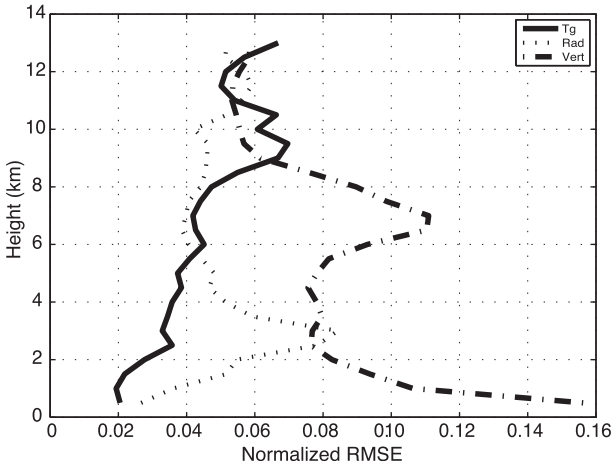

FIG. 6. Evolution of the normalized RMSE with height for the tangential wind (solid), the radial wind (dotted), and the vertical wind (dash–dotted).

than that of the horizontal components except at altitude higher than 9 km, where all the curves converge.

b. Storm structure evaluation

The azimuthal mean of the primary and secondary circulations is now evaluated, as well as characteristics such as boundary layer height, wind radii, etc. To better understand the following evaluation of storm structure, it is important to first have a quantitative knowledge of the amount of data ''observed'' by the radar in both the vertical and radial directions. Figure 7 shows the radial-height profile distribution of data ''observed'' by the radar. This figure reveals areas of missing data caused by a lack of simulated reflectors. During the simulated data collection, at most altitudes, only 20% or less of the wind data was sampled within 25 km of the center. The largest amount of data sampled by the radar is confined to the lowest 8 km between 30 and 80 km from the storm center.

Figure 8 is a radial-height azimuthal mean (hereafter *R–Z* mean) profile of tangential wind, illustrating an accurate retrieval of the vertical structure of the storm by the analysis. The tilt of the eyewall is well captured, and the position of the maximum seems qualitatively accurate. A quantitative assessment of the position and the magnitude of the maximum tangential wind are shown in Figs. 9 and 10, respectively. Data are not plotted when the maximum tangential wind could not be computed because of missing data. Figure 9 shows a comparison of the radius of maximum wind (RMW) at all heights (Fig. 9a) and the associated error (Fig. 9b). The radius of the maximum mean azimuthal wind is quite well retrieved up to ~8 km MSL, where the error is in general small (<6 km), and above 8 km MSL there are large departures from the truth, where over 60% of data are missing (Fig. 7). Comparison of the maximum tangential wind (Fig. 10) indicates a relatively small underestimation in the analysis below 3 km MSL. From there up to 8 km MSL, the maxima are nearly equal to each other. Further up in the troposphere, larger departures occur.

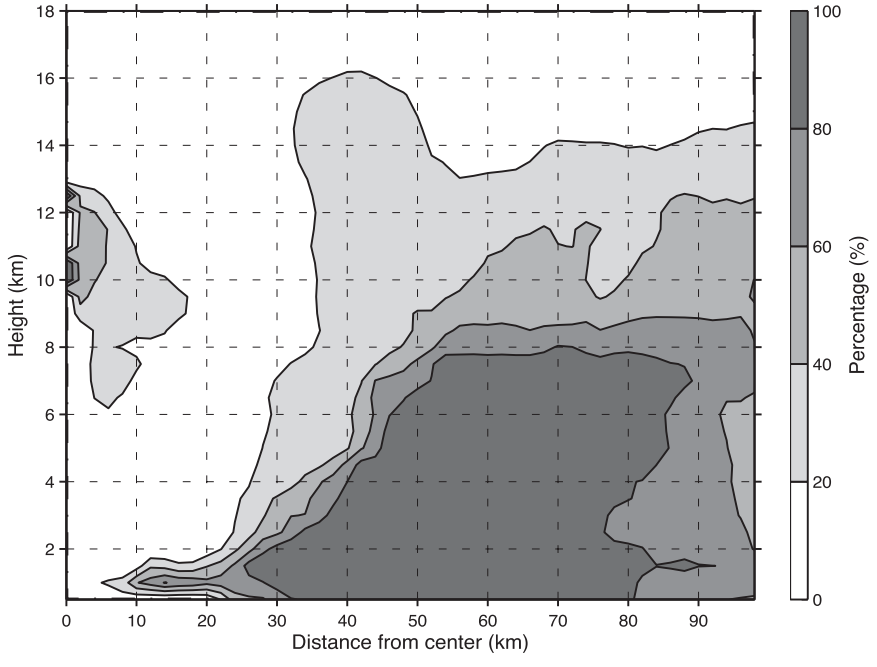

FIG. 7. Vertical distribution of ''observed'' data in the truth due to thresholding on CWC.

Unauthenticated | Downloaded 04/25/25 07:24 PM UTC

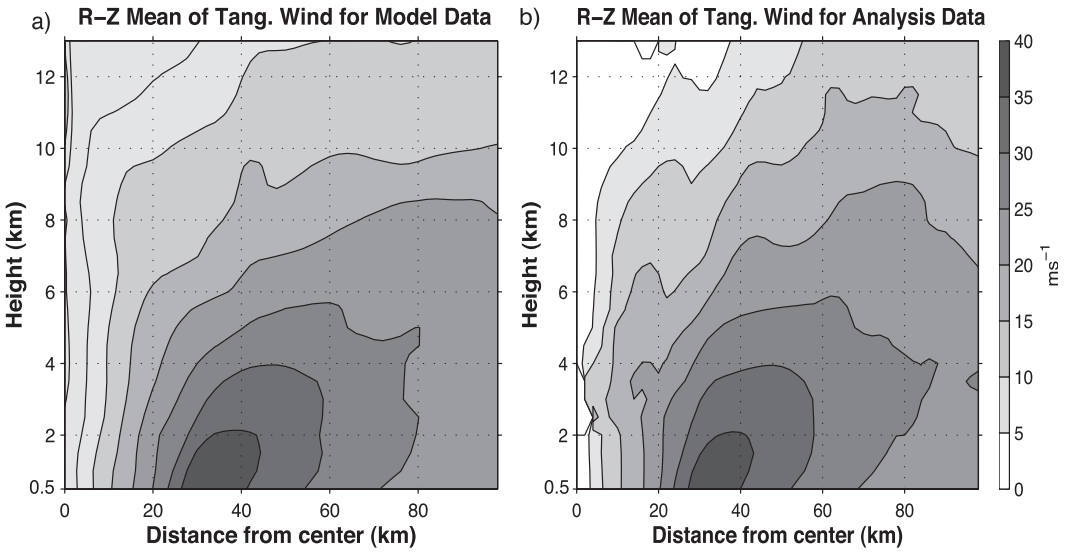

FIG. 8. Tangential wind *R–Z* mean.

Wind radii are usually used to diagnose the size of a TC. Table 1 summarizes the comparison between the hurricane-force wind (33 m s^{-1}) radius in the truth and the analysis at the three lowest levels and shows that storm size is well retrieved in the analysis. The vertical structure of the radial wind is also very important to provide critical information on the structure of the secondary circulation in a TC. Figure 11 documents the *R–Z* mean radial wind for both the truth and the radar analysis. The vertical structure of the radial wind is mostly well retrieved by the analysis data. The inflow layer and its depth are accurately estimated. The mid-level outflow in the outer range of the domain, although a bit underestimated in magnitude, is also well depicted. Meanwhile, the magnitude of the upper-level outflow is slightly overestimated. These kinematic features are relatively well represented considering the amount of data actually sampled by the radar (Fig. 7). Inside the eye, where ''reflectors'' are practically nonexistent, the retrieval is more problematic, as was already suggested in horizontal cross sections (Fig. 4). The upper-level outflow at 30–50 km from the center is much stronger in the analysis, reinforcing the large departure seen above 8 km MSL. The outflow immediately above the inflow layer in the area near the RMW is not well analyzed, which is likely because this outflow layer is thin and might not be well sampled (Fig. 7). The maximum inflow in the truth (4.5 m s^{-1}) is slightly overestimated in the analysis (5.0 m s^{-1}) but is at the correct height (500 m) and is within 2 km radially. A second inflow region (70 km $< r <$ 100 km) is retrieved less accurately in the analysis. The inflow magnitude in this region is 4.6 compared to 6.9 m s^{-1} in the analysis. The height of the top of the inflow layer (Fig. 11, thick black lines), defined as the height at which the inflow magnitude is 10% of the maximum inflow magnitude (J. A. Zhang et al. 2011), is a very important characteristic of the vertical structure of the TC boundary layer. The retrieved inflow depth is relatively accurate except inside the 25-km radius and near the domain boundary, and the error never exceeds two vertical grid points (1 km in each case).

The mean azimuthal structure of the vertical wind component is also evaluated, as it is also an important part of the secondary circulation. It can provide crucial information on the strength of convection and thus can help identify whether a TC is going through intensification. Figure 12 shows the *R–Z* mean of the vertical wind for both truth and analysis data. As for the radial wind, the analysis exhibits large departures from the truth inside the eye ($r <$ 25 km) and above 8 km MSL. Although the main updraft is well retrieved and at the correct position, it does not extend down to the lowest level as seen in the truth. The updraft is also overestimated in the analysis by 1–3 m s^{-1} at higher levels. Near the surface, the downdraft is somewhat overestimated.

Finally, the storm structure is analyzed in the azimuthal spectral domain, as such analysis reveals the asymmetric kinematic structure of a TC. Extracting the different wavenumbers of an observed signal is often challenging as missing data, low temporal resolution, low spatial resolution, or a short time window of acquisition can severely impede the spectral decomposition (Lorsolo and Aksoy 2012). A wavenumber decomposition of the wind is performed similar to the technique documented in Marks et al. (1992). Wavenumbers 0 and 1 are extracted and analyzed. Here, wavenumber 0 retrieval

Unauthenticated | Downloaded 04/25/25 07:24 PM UTC

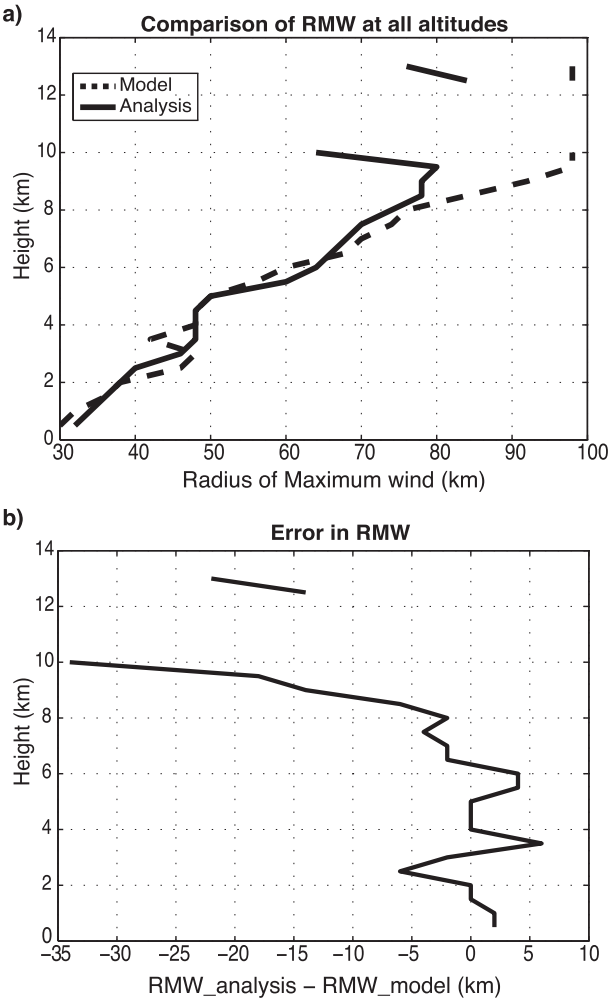

FIG. 9. Evolution of RMW with (a) height and (b) associated error.

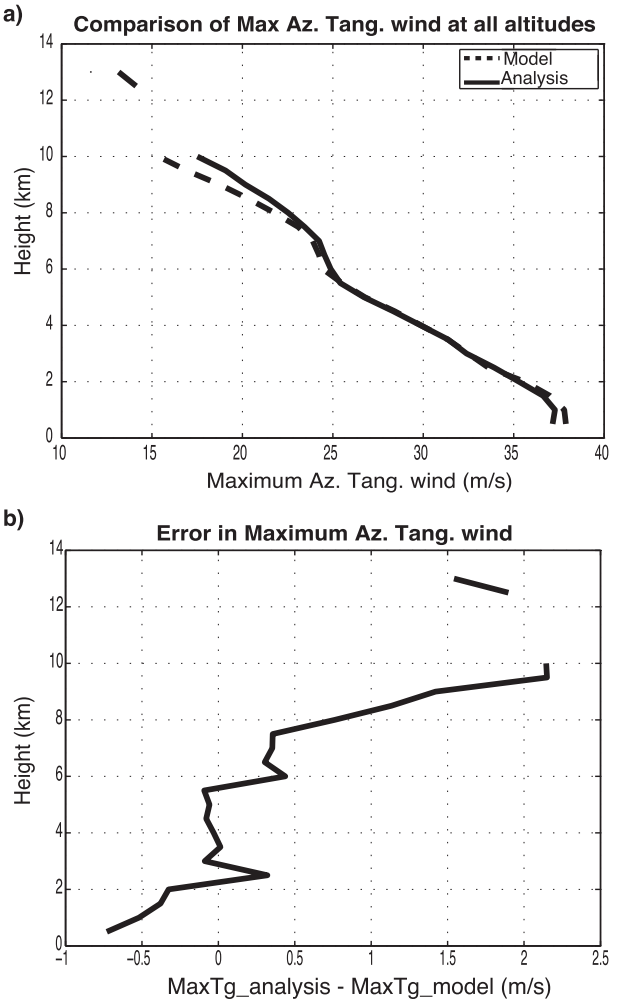

FIG. 10. Evolution of the maximum tangential wind with (a) height and (b) associated error.

is quantitatively assessed and wavenumber 1 is qualitatively evaluated at altitudes where the issue of missing data is not significant. Figure 13 shows a comparison of wavenumber 0 at 1 km MSL for the horizontal components. The comparison of the amplitude of the wavenumber 0 for the tangential wind is very accurate (99% variance explained). A similar evaluation for the radial wind is somewhat less accurate but still of good quality (91% variance explained). The amplitude of wavenumber 0 for the radial wind is, however, overestimated. Figure 14 shows a comparison of wavenumber 1 for the tangential and radial wind at 1-km altitude and at 2.5 km for the vertical wind component. Qualitatively, there is a negligible phase shift in the analysis in areas where the retrieval was relatively accurate. In the cases of tangential and radial components of the wind, the magnitude is slightly lower than in the truth. Comparison of wavenumber 1 for the vertical wind shows rather encouraging results. There is good agreement for both the phase and the amplitude in the 20–30-km ring. Beyond the 30-km radius, there is still a good agreement in magnitude but there is a 45° phase shift between the two fields. A better understanding of these discrepancies would require the use of the method described in Lorsolo and Aksoy (2012) and is beyond the scope of this study. For all three components, the wavenumber retrieval is not reliable in areas with little amounts of data (e.g., inside the eye).

TABLE 1. Hurricane wind radii at 0.5, 1, and 1.5 km MSL.

	Truth (km)	Analysis (km)
0.5	45.9	44.2
1.0	48.4	46.9
1.5	49.7	48.8

Unauthenticated | Downloaded 04/25/25 07:24 PM UTC

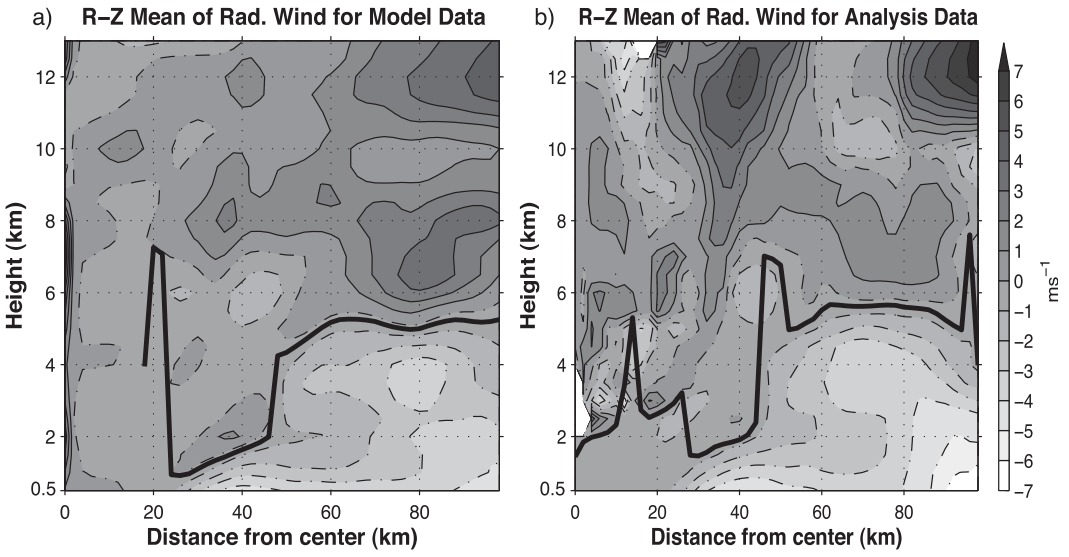

FIG. 11. As in Fig. 8, but for the radial wind component. The thick black line represents the top of the inflow layer. Solid and dashed lines represent positive and negative values of the radial wind, respectively.

4. Error sources and impact of simplifications in the methodology

The goal of the present study is to assess the performance of the HRD analysis software in a context where most of the errors that arise during the collection of observations themselves are eliminated, so that errors in the software itself are better isolated. However, in practice, there are many sources of error in a three-dimensional wind analysis. Generally, errors arise from 1) the smoothing inherent in the averaging of return within the width of the radar beam; 2) missing data, including data rejected because of (i) insufficient signal-to-noise ratio, (ii) blocking from intervening attenuation by precipitation that reduces the signal-to-noise ratio unacceptably, (iii) contamination by scattering of the main lobe by the sea surface, and (iv) contamination by scattering of the sidelobe by the sea surface; 3) the method of interpolation of data to the grid; 4) solution of the discretized three-dimensional continuity equation on the grid; 5) smoothing introduced by the second-derivative filter in the least squares solution; 6) the correction of the Doppler radials for fall speed of the precipitation relative to the air motion using an assumed fall speed–reflectivity relationship; 7) errors in the air motion at the boundary; and 8) systematic pointing

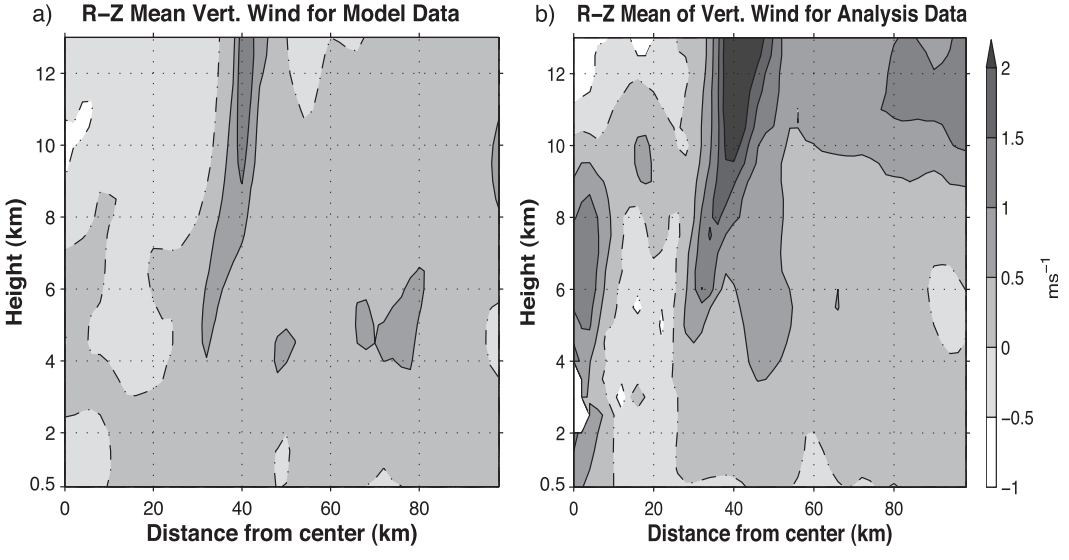

FIG. 12. As in Fig. 8, but for the vertical wind component.

Unauthenticated | Downloaded 04/25/25 07:24 PM UTC

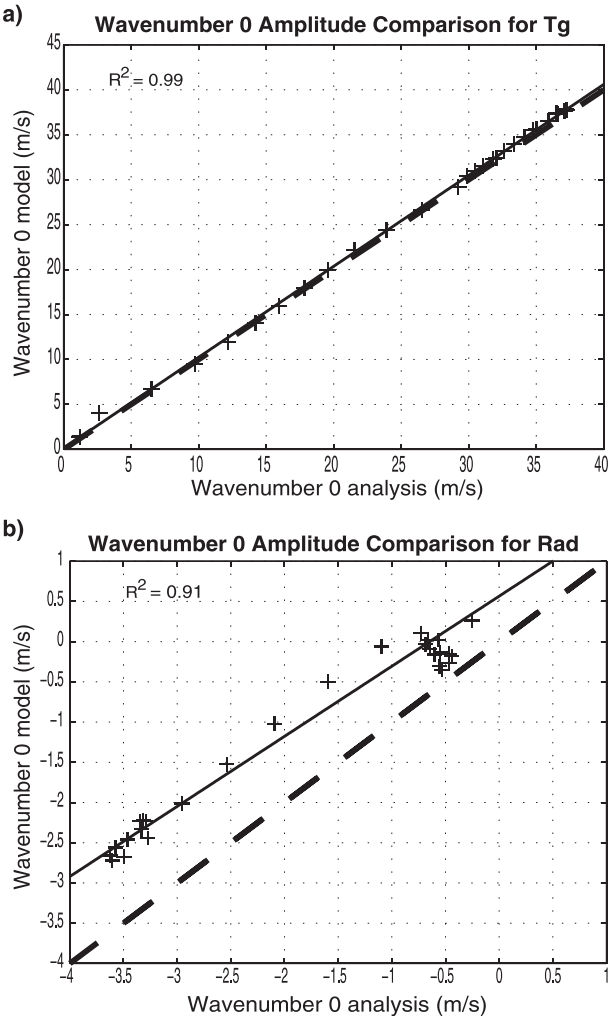

FIG. 13. Comparison of wavenumber 0 magnitude (m s^{-1}) for the (a) tangential wind and (b) radial wind. Thin solid line represents the linear fit, and thick dashed line indicates the 1:1 line.

errors of the Doppler radar resulting from errors in measurement of the mounting on the aircraft, as well as errors in the pitch drift and roll. Other errors in the radial and tangential winds result from an inaccurate determination of the center; however, in this study the same center is used for the model and analysis grids.

The errors evaluated in this investigation are 2(i), 3–5, and 7, as they represent errors from the software itself. Error sources that are omitted are as follows: Beamwidth is not used in the sampling of the model wind output (error 1). Data are included down to the surface since there is no attempt to model sea surface scattering [error 2(iii)], and there is no attempt to model sidelobe sea surface scattering [error 2(iv)]. The sampling is directly of the total wind field so there is no error due to fall speed (error 6). Error 2(i) is addressed by only including Doppler radials where the model indicated sufficient condensate. Errors 3 and 4 are inherent in the process of interpolating to a grid and running the three-dimensional least squares solution. In tests of the least squares solution using analytic functions, it can be seen that the error is quite small (Gamache 1997); however, higher-frequency spectral components in real data and real wind fields increase errors in any solution involving a discretized continuity equation (Gamache 1997). These tend to be mitigated by the second-derivation smoother. When considering the actual beamwidth, the resulting smoothing will tend to reduce small-scale and wind gradient resolutions.

In a real situation, blocking of the X-band signal by the eyewall can be substantial, and scattering by the sea surface of the main lobe and sidelobes [errors 2(iii) and 2 (iv)] can be quite intense in a hurricane. This increases particularly the amount of data missing in the very important boundary layer, especially farther from the aircraft track, as the beam widens with distance. These missing precipitation effects can be very difficult to assess quantitatively, except by modeling them, which will be done in follow-up studies. The only missing-precipitation error we can estimate fairly realistically is the absence of data in precipitation-free volumes.

Some error in the three-dimensional solution may also be expected from the high weight given to the mass continuity equation in the cost function. This is necessary, since examination of the continuity solution near the flight track contained nonrandom error of the same sign over numerous contiguous grid points.

The weak value of the boundary conditions can also cause error, while possibly mitigating others. Strong boundary conditions at the surface are not reasonable, since so many factors can increase the lower boundary of radial–velocity data, and errors in boundary layer vertical wind and convergence will propagate upward.

The errors associated with fall speed are also not included in the analysis, since the synthetic Doppler radials were derived from the air motion and not from precipitation motion. Based upon other experience in hurricanes, we expect the biases and random errors in the fall speed near flight level to be 1–2 and 2–3 m s^{-1}, respectively (Black et al. 1996). Hail has not been sampled during aircraft penetrations of hurricanes over the ocean, so much larger fall speed errors are not likely. Occasional larger errors, where rain or frozen drops reach above 10 km, might approach 10 m s^{-1} due to decreasing density, but these are rare in hurricane penetrations. These errors will affect the vertical motion directly above and below the aircraft, while the effect on the three-dimensional horizontal wind solution arising from fall speed errors in radar radial velocity is more difficult to assess except by future modeling.

Unauthenticated | Downloaded 04/25/25 07:24 PM UTC

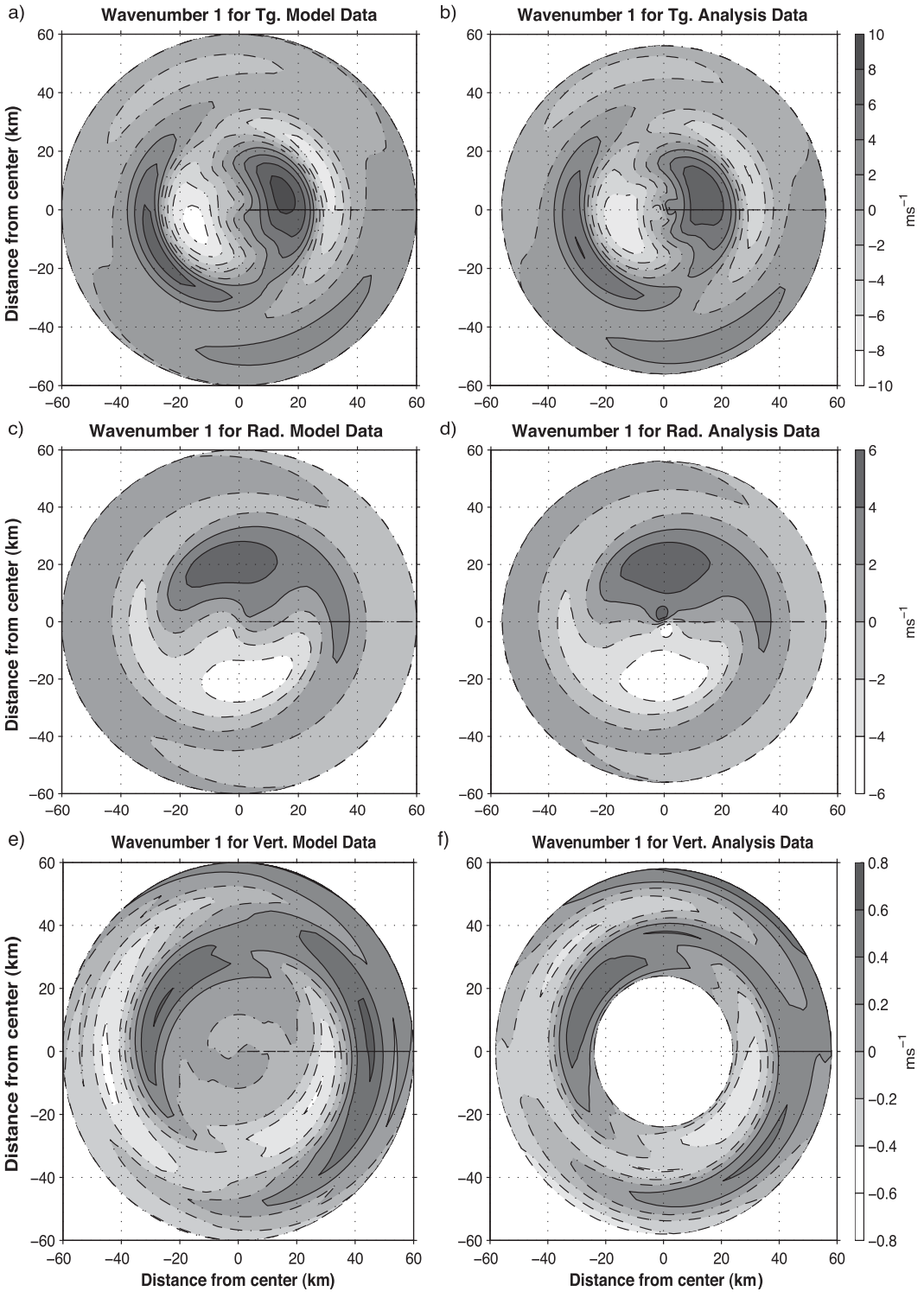

FIG. 14. Wavenumber 1 at 1 km MSL for the (a) tangential, (b) radial, and at 2.5 km for (c) vertical wind components for (left) truth and (right) analysis.

Unauthenticated | Downloaded 04/25/25 07:24 PM UTC

If no attempt is made to correct for navigation errors, then systematic biases as large as 2–3 m s^{-1} can occur from errors in the measurement of the mounting of the antenna, particularly the tilt angle relative to the plane perpendicular to the fuselage. Other more random errors, of a similar magnitude, can occur as a result of errors in measurement of aircraft pitch, drift, roll, and motion. After careful determination, using the method of Testud et al. (1995), biases resulting from errors in antenna mounting angles can be expected to be reduced to under 1 m s^{-1}, but the random errors due to aircraft attitude measurements may remain as high as 2–3 m s^{-1}.

One final source of error in the continuity equation solution is possible, and it may explain the bias in tangential wind above and below flight level. Immediately above and below the aircraft, the tangential wind is essentially determined by the integration of the continuity equation, since there is little or no projection of the horizontal wind upon the Doppler radial, and the characteristic direction of integration is essentially perpendicular to the coplanes and therefore horizontal, not vertical. Thus, the horizontal wind determined from either side of the plane of the flight track, together with the continuity equation, helps to determine the tangential wind above the flight track. Since the characteristic of integration of continuity near the aircraft intersects the surface very obliquely or not at all, there is little or no explicit constraint on the constant of integration of mass continuity in the circle around the flight track. Thus, any error in the constant of integration would produce errors in the cross-track (tangential when the aircraft flies storm-radial legs) wind of opposite signs above and below flight level. Fortunately, the solution of the problem is improved by the fact that one large three-dimensional cost function is minimized, and that cost function includes the second-derivative constraint and projection equations. Nevertheless, a small constant-of-integration error may help to explain the opposite sign bias in tangential wind above and below flight level.

5. Conclusions

The present study extends the work of Gamache (1997) by performing an in-depth evaluation of the HRD radar analysis software using a realistic simulated TC. Doppler radar data simulated from a model run are processed with the analysis software and the three components of the wind are retrieved. The obtained analysis is then compared to the original ''truth'' model wind field.

Comparison of the two datasets shows that, in general, the retrieval is of very good quality up to ~8-km height, the volume where good data coverage results in small error in retrieved winds. The analyses accurately capture the wind field's main characteristics as well as smaller-scale features. At higher levels, retrieval of the wind becomes more challenging because of large areas not being sampled. The tangential wind is found to be the best retrieved component, but retrieval of the radial wind component is also quite accurate, as confirmed by low RMSE values. The tangential wind retrieval exhibits a noticeable negative bias below the flight level and a positive bias above, while the radial wind mostly exhibits a positive bias. Although theses biases are found to be rather small, they are nevertheless statistically significant. The software provides a fairly decent analysis of the vertical motion, where updraft and downdraft are, in general, spatially well represented. Unlike the horizontal components, the vertical wind component is best retrieved at midlevels, as illustrated by the normalized RMSE.

Examination of the vortex structure computed from the analysis shows a rather accurate retrieval of the main TC features. The wind maxima at various levels and the RMW are retrieved with very good accuracy, in the tangential *R–Z* mean. The *R–Z* mean of radial wind displays a faithful representation of the main inflow, although the outflow jet usually present at the top of the inflow is somewhat underestimated here, probably because sampling resolution issues and the analysis method (analysis resolution, smoothing). The *R–Z* mean of the vertical wind component provides encouraging results, with the main updraft being well represented; however, there are a few issues at low levels, which might be due to more missing data and the boundary conditions in the continuity assumption. A quick study of the low wavenumbers of the horizontal wind components shows that, in general, there is little phase error between the fields. Wavenumber 1 for the vertical wind component displays larger phase error at larger radii. The magnitude of the wavenumbers is, in general, lower in the analysis than in the truth field.

This evaluation provides a good assessment of the retrieved wind obtained using the HRD analysis software. The use of realistic data, while using some sampling simplifications (no terminal velocity, no advection due to non-simultaneity of data, etc.), allows a first-order assessment of the software. To better understand how best to use and interpret the analysis, a discussion of the sources of error in a three-dimensional analysis and of the effect of the simplifications made to simulate the data is also provided. A follow-up study will focus on ways to improve the algorithm by conducting sensitivity tests when these other types of errors are considered. The quality of the retrieval will also be tested when different interpolation schemes are applied or when the radius of influence is varied. Performing the computation on a polar grid, more natural to the hurricane problem, will also be tested.

Unauthenticated | Downloaded 04/25/25 07:24 PM UTC

Acknowledgments. The authors acknowledge funding from the NOAA Hurricane Forecast Improvement Project that supported this work. This research was carried out (in part) under the auspices of CIMAS, a joint institute of the University of Miami and NOAA, Cooperative Agreement NA67RJ0149. The authors thank Dr. Paul Reasor and the anonymous reviewers for their insightful input.

REFERENCES

Aksoy, A., S. Lorsolo, T. Vukicevic, K. Sellwood, S. Aberson, and F. Zhang, 2012: The HWRF Hurricane Ensemble Data Assimilation System (HEDAS) for high-resolution data: The impact of airborne Doppler radar observations in an OSSE. *Mon. Wea. Rev.,* **140,** 1843–1862.

Black, M. L., R. W. Burpee, and F. D. Marks Jr., 1996: Vertical motion characteristics of tropical cyclones determined with airborne Doppler radial velocities. *J. Atmos. Sci.,* **53,** 1887–1909.

Bosart, B. L., W.-C. Lee, and R. M. Wakimoto, 2002: Procedures to improve the accuracy of airborne Doppler radar data. *J. Atmos. Oceanic Technol.,* **19,** 322–339.

Bousquet, O., and M. Chong, 1998: A Multiple-Doppler Synthesis and Continuity Adjustment Technique (MUSCAT) to recover wind components from Doppler radar measurements. *J. Atmos. Oceanic Technol.,* **15,** 343–359.

Dodge, P., R. W. Burpee, and F. D. Marks, 1999: The kinematic structure of a hurricane with sea level pressure less than 900 mb. *Mon. Wea. Rev.,* **127,** 987–1004.

Gamache, J. F., 1997: Evaluation of a fully three-dimensional variational Doppler analysis technique. Preprints, *28th Conf. on Radar Meteorology,* Austin, TX, Amer. Meteor. Soc., 422–423.

——, F. D. Marks Jr., and F. Roux, 1995: Comparison of three airborne Doppler sampling techniques with airborne in situ wind observations in Hurricane Gustav (1990). *J. Atmos. Oceanic Technol.,* **12,** 171–181.

Gao, J., M. Xue, A. Shapiro, and K. K. Droegemeier, 1999: A variational method for the analysis of three-dimensional wind fields from two Doppler radars. *Mon. Wea. Rev.,* **127,** 2128–2142.

Gopalakrishnan, S. G., F. Marks Jr., X. Zhang, J.-W. Bao, K.-S. Yeh, and R. Atlas, 2011: The experimental HWRF system: A study on the influence of horizontal resolution on the structure and intensity changes in tropical cyclones using an idealized framework. *Mon. Wea. Rev.,* **139,** 1762–1784.

Hildebrand, P. H., and C. K. Mueller, 1985: Evaluation of meteorological airborne Doppler radar. Part I: Dual-Doppler analyses of air motions. *J. Atmos. Oceanic Technol.,* **2,** 362–380.

Jorgensen, D. P., and J. D. DuGranrut, 1991: A dual-beam technique for deriving wind fields from airborne Doppler radar. Preprints, *25th Int. Conf. on Radar Meteorology,* Paris, France, Amer. Meteor. Soc., 458–461.

——, P. H. Hildebrand, and C. L. Frush, 1983: Feasibility test of an airborne pulse-Doppler meteorological radar. *J. Climate Appl. Meteor.,* **22,** 744–757.

——, T. Matejka, and J. DuGranrut, 1996: Multi-beam techniques for deriving wind fields from airborne Doppler radars. *Meteor. Atmos. Phys.,* **59,** 83–104.

Lee, W.-C., P. Dodge, F. D. Marks Jr., and P. H. Hildebrand, 1994: Mapping of airborne Doppler radar data. *J. Atmos. Oceanic Technol.,* **11,** 572–578.

——, F. D. Marks, and C. Walther, 2003: Airborne Doppler radar data analysis workshop. *Bull. Amer. Meteor. Soc.,* **84,** 1063–1075.

Lhermitte, R. M., 1971: Probing of atmospheric motion by airborne pulse-Doppler radar techniques. *J. Appl. Meteor.,* **10,** 234–236.

Lorsolo, S., and A. Aksoy, 2012: Wavenumber analysis of azimuthally distributed data: Assessing maximum allowable gap size. *Mon. Wea. Rev.,* **140,** 1945–1956.

——, J. Zhang, F. D. Marks, and J. Gamache, 2010: Estimation and mapping of hurricane turbulent energy using airborne Doppler measurements. *Mon. Wea. Rev.,* **138,** 3656–3670.

Marks, F. D., Jr., 2003: State of the science: Radar view of tropical cyclones. *Radar and Atmospheric Science: A Collection of Essays in Honor of David Atlas, Meteor. Monogr.,* No. 30, Amer. Meteor. Soc., 33–74.

——, and R. A. Houze Jr., 1984: Airborne Doppler radar observations in Hurricane Debby. *Bull. Amer. Meteor. Soc.,* **65,** 569–582.

——, and ——, 1987: Inner core structure of Hurricane Alicia from airborne Doppler radar observations. *J. Atmos. Sci.,* **44,** 1296–1317.

——, ——, and J. F. Gamache, 1992: Dual-aircraft investigation of the inner core of Hurricane Norbert. Part I: Kinematic structure. *J. Atmos. Sci.,* **49,** 919–942.

Ray, P. S., and D. P. Jorgensen, 1988: Uncertainties associated with combining airborne and ground-based Doppler radar data. *J. Atmos. Oceanic Technol.,* **5,** 177–196.

——, and M. Stephenson, 1990: Assessment of the geometric and temporal errors associated with airborne Doppler radar measurements of a convective storm. *J. Atmos. Oceanic Technol.,* **7,** 206–217.

——, C. L. Ziegler, W. Bumgarner, and R. J. Serafin, 1980: Single- and multiple-Doppler radar observations of tornadic storms. *Mon. Wea. Rev.,* **108,** 1607–1625.

Reasor, P. D., M. T. Montgomery, F. D. Marks Jr., and J. F. Gamache, 2000: Low-wavenumber structure and evolution of the hurricane inner core observed by airborne dual-Doppler radar. *Mon. Wea. Rev.,* **128,** 1653–1680.

——, M. D. Eastin, and J. F. Gamache, 2009: Rapidly intensifying Hurricane Guillermo (1997). Part I: Low-wavenumber structure and evolution. *Mon. Wea. Rev.,* **137,** 603–631.

Rogers, R., and Coauthors, 2006: The Intensity Forecasting Experiment: A NOAA multiyear field program for improving tropical cyclone intensity forecasts. *Bull. Amer. Meteor. Soc.,* **87,** 1523–1537.

——, S. Lorsolo, P. Reasor, J. Gamache, and F. Marks, 2012: Multiscale analysis of tropical cyclone kinematic structure from airborne Doppler radar composites. *Mon. Wea. Rev.,* **140,** 77–99.

Stern, D. P., and D. S. Nolan, 2009: Reexamining the vertical structure of tangential winds in tropical cyclones: Observations and theory. *J. Atmos. Sci.,* **66,** 3579–3600.

Testud, J., P. H. Hildebrand, and W. Lee, 1995: A procedure to correct airborne Doppler radar data for navigation errors using the echo returned from the Earth's surface. *J. Atmos. Oceanic Technol.,* **12,** 800–820.

Wakimoto, R. M., W.-C. Lee, H. B. Bluestein, C.-H. Liu, and P. H. Hildebrand, 1996: ELDORA observations during VORTEX 95. *Bull. Amer. Meteor. Soc.,* **77,** 1465–1481.

Zhang, J. A., R. F. Rogers, D. S. Nolan, and F. D. Marks, 2011: On the characteristic height scales of the hurricane boundary layer. *Mon. Wea. Rev.,* **139,** 2523–2535.

Zhang, X., T. S. Quirino, K.-S. Yeh, S. G. Gopalakrishnan, F. D. Marks Jr., S. G. Goldenberg, and S. D. Aberson, 2011: HWRFx: Toward improving hurricane forecasts with high-resolution modeling. *Comput. Sci. Eng.,* **13,** 13–21.

Unauthenticated | Downloaded 04/25/25 07:24 PM UTC